JACS
JOURNAL OF THE AMERICAN CHEMICAL SOCIETY
pubs.acs.org/JACS
Article

Molecular Oxygen-Induced Ferromagnetism and Half-Metallicity in α-$BaNaO_4$: A First-Principles Study

Jun Deng, Jiangang Guo,* and Xiaolong Chen*

Cite This: J. Am. Chem. Soc. 2020, 142, 5234−5240
Read Online

ACCESS | Metrics & More | Article Recommendations | Supporting Information

Downloaded via INST OF PHYSICS on March 25, 2020 at 07:13:23 (UTC).
See https://pubs.acs.org/sharingguidelines for options on how to legitimately share published articles.

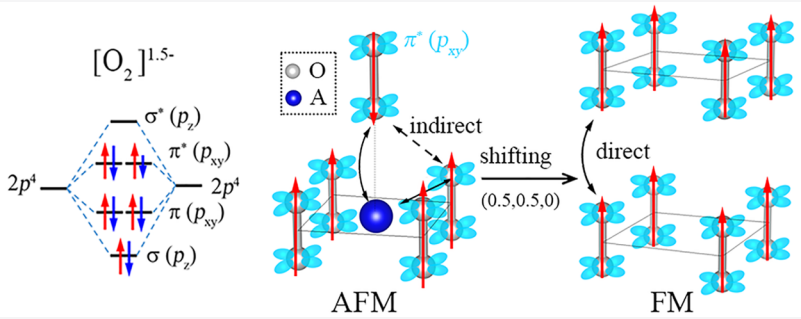

ABSTRACT: Molecular oxygen resembles 3*d* and 4*f* metals in exhibiting long-range spin ordering and strong electron correlation behaviors in compounds. Ferromagnetic spin ordering and half-metallicity, however, are quite elusive and have not been well acknowledged. In this Article, we address this issue by studying how spins will interact with each other if the oxygen dimers are arranged in a different way from that in the known superoxides and peroxides by first-principles calculations. Based on the results of a structure search, thermodynamic studies, and lattice dynamics, we show that tetragonal α-$BaNaO_4$ is a stable half-metal with a Curie temperature at 120 K, the first example in this class of compounds. Like 3*d* and 4*f* metals, the O_2 dimer carries a local magnetic moment of 0.5 μ_B due to the unpaired electrons in its π^* orbitals. This compound can be regarded as forming from the O_2 dimer layers stacking in a head-to-head way. In contrast to the arrangement in AO_2 (A = K, Rb, Cs), the spins are ferromagnetically coupled both within and between the layers. Spin polarization occurs in π^* orbitals, with spin-up electrons fully occupying the valence band and spin-down electrons partially occupying the conduction band, forming semiconducting and metallic channels, respectively. Our results highlight the importance of geometric arrangement of O_2 dimers in inducing ferromagnetism and other novel properties in O_2-dimer-containing compounds.

■ INTRODUCTION

Molecular oxygen (O_2) has long been known to carry a local moment because of the existence of unpaired electron in its π^* orbitals.[1] When condensing into a solid at low temperatures (∼24 K), it exhibits a long-range antiferromagnetic (AFM) ordering.[2,3] Alkali metal superoxides (O_2^-), peroxides (O_2^{2-}), and dioxygenyl (O_2^+) salts all contain molecular oxygen but with different numbers of electrons in their π^* orbitals, leading to a variety of magnetic properties. Typical examples are AFM AO_2 (A = Na, K, Rb, Cs),[4−9] spin-glass Rb_4O_6/Cs_4O_6,[10,11] ferrimagnetic (FiM) O_2PtF_6,[12,13] and paramagnetic O_2SbF_6.[13] Long-range ferromagnetic (FM) ordering, however, is quite elusive in these O_2-dimer-containing compounds, though many attempts have been made to study it over the past decades.

A weak ferromagnetism was reported in $Ba_{1-x}K_xO_2$ for x = 0.269, and a spin-glass behavior for other K doping levels, which were ascribed to the coexistence of and the competition between AFM and FM.[14,15] Partial oxygen deficiency at x = 0.28 in RbO_{2-x} was found to result in a transition from AFM to spin-glass, and presumably there is short-range FM ordering in clusters at ∼50 K.[16] Theoretically, the electrons in the π^* orbitals of O_2 dimers can be better treated as a strongly correlated system.[17,18] Naghavi et al. predicted that pressure would make Rb_4O_6 transform from an AFM insulator to an FM insulator then to an FM half-metal, which is a consequence of Mott transitions.[19] It is argued from first-principles calculations that anionogenic ferromagnetism and half-metallicity will emerge at the interface of KO_2/BaO_2 through double-exchange interactions of O_2^{2-} and O_2^-.[20] A question arises: Is long-range FM ordering possible in a bulky molecular oxygen-containing compound, as it is in a 3*d* metal counterpart? If so, can a half-metal be evolved from the

Received: December 10, 2019
Published: February 21, 2020

© 2020 American Chemical Society

https://dx.doi.org/10.1021/jacs.9b13295
J. Am. Chem. Soc. 2020, 142, 5234−5240

ferromagnetism? This is of importance in further understanding the interaction behavior among these local moments carried by O_2 dimers.

To begin, we first show the importance of O_2 dimer orientation in inducing long-range ordering by taking Rb_4O_6 and RbO_2 as examples; see Figure 1a,b. The O_2 dimers in

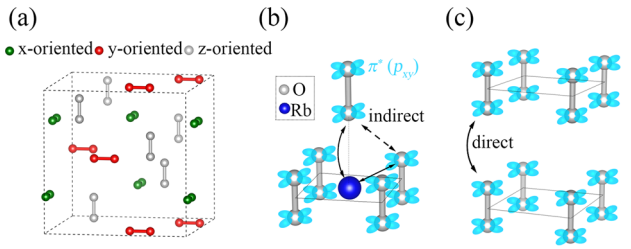

Figure 1. (a) Sketch of arrangement of O_2 dimers in Rb_4O_6. For simplification, all the cations are omitted. (b, c) Orbital-based schematic diagrams of (b) indirect magnetic interaction between the O_2 dimers in RbO_2 and (c) hypothetical direct magnetic interaction between the O_2 dimers. The magnetic interactions originate from the unfilled $\pi^*(p_{xy})$ orbitals (blue).

Rb_4O_6 align on three principal axes. Due to geometric frustration, it does not show long-range magnetic ordering.[10] In contrast, the ground state of RbO_2 is experimentally confirmed to be AFM,[5] for all the O_2 dimers align parallel. The O_2 dimers couple ferromagnetically in the (001) planes in RbO_2 while interacting antiferromagnetically between adjacent planes with a relative shift of (0.5*a*, 0.5*a*, 0), where *a* is the lattice parameter. Both magnetic exchange interactions are theoretically found to be indirect, i.e., via the cations through superexchnage.[21] The same is true for AFM KO_2 and CsO_2.[4] These facts suggest that the O_2 dimer layers in such a stacking way favor the AFM interlayer exchange interactions for local moments. Recent studies showed that changes in the relative orientation of layers will give rise to tremendous changes in electronic properties and hence result in emergent phenomena.[22] We try to apply this idea to the O_2-dimer-containing compounds to explore how their magnetic properties will change—specifically, rearranging the relative orientation of neighboring O_2 dimer layers while keeping the intralayer unchanged. Figure 1c shows a possible simple solution, where the O_2 dimers stack along the [001] direction in a head-to-head way. In this way, the O_2 dimers in neighboring planes are expected to have direct exchange interactions and bring about very different magnetic properties.

Since no known binary peroxides and superoxides have such an O_2 arrangements in their structures, ternary compounds should be considered. However, very few ternary peroxides or superoxides have been reported so far. The substitution of K for Ba in BaO_2 only leads to a solid solution, without changing the structure type.[14] This is not beyond expectation, since K^+ ion and Ba^{2+} ion are comparable in size. The desired structure is more likely to form if a smaller ion, say Na^+, is used instead.

In this Article, we report attempts to identify α-$BaNaO_4$ in which the O_2 dimers arrange in the way shown in Figure 1c among the predicted compounds by performing a systematic structure search. This compound is stable in terms of formation enthalpy, mechanical dynamics, and lattice dynamics. It exhibits ferromagnetism and half-metallicity, with a large spin gap ~4 eV (HSE06) in the ground state. The emergent half-metallicity is attributed to the partial occupation of the O_2 dimer π^* bonds, which leads to the spin splitting. Monte Carlo simulations based on the Heisenberg model indicate that the spin ordering occurs at a Curie temperature (T_c) of 120 K. Our results show that compounds with adjacent O_2 dimer layers stacking in a head-to-head way are possible and may change the interlayer coupling from AFM to FM, highlighting the importance of the relative shift of adjacent layers in inducing novel properties for this category of compounds.

■ COMPUTATIONAL DETAILS

First-principles calculations were carried out with the density functional theory (DFT) implemented in the Vienna *ab initio* simulation package (VASP).[23] We adopted the generalized gradient approximation (GGA) in the form of Perdew−Burke−Ernzerhof (PBE)[24] for the exchange-correlation potentials. The projector-augmented-wave (PAW)[25] pseudopotentials were used with a plane wave energy of 680 eV; $2s^22p^4$, $2p^63s^1$, and $5s^25p^66s^2$ were treated as valence electrons for O, Na, and Ba, respectively. A Monkhorst−Pack[26] Brillouin zone sampling grid with a resolution 0.02 $\times 2\pi$ Å^{-1} was applied. Atomic positions and lattice parameters were relaxed

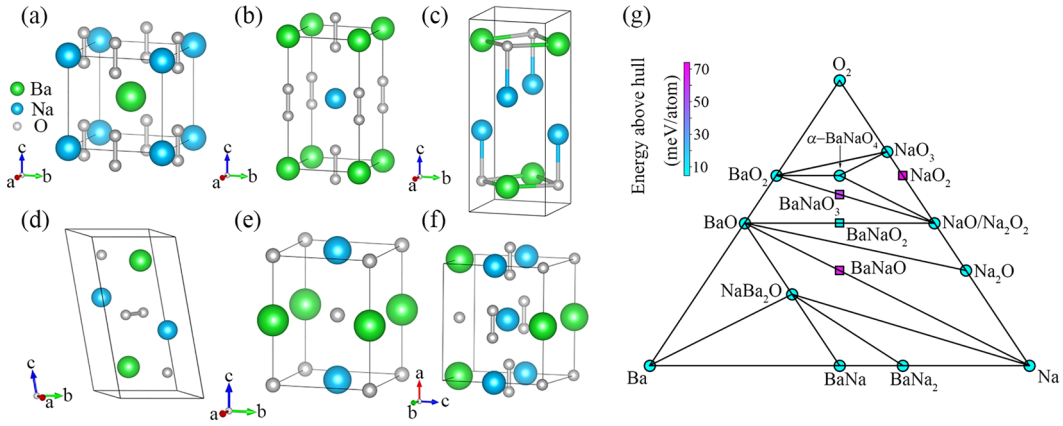

Figure 2. Crystal structures of (a) *P*4/*mmm*-$BaNaO_4$ (α-$BaNaO_4$), (b) *P*4/*mmm*-$BaNaO_4$ (β-$BaNaO_4$), (c) *P*4/*nmm*-BaNaO, (d) $P\bar{1}$-$BaNaO_2$, (e) *P*4/*mmm*-$BaNaO_2$, and (f) *Pmmn*-$BaNaO_3$. Green balls represent barium, blue ones sodium, and gray dumbbells O_2 dimer. (g) Phase diagram based on convex hull analysis of formation enthalpies for the Ba-Na-O system at T = 0 K. Formation enthalpy ΔH was defined as $\Delta H_{Ba_xNa_yO_z} = E_{Ba_xNa_yO_z} - xE_{Ba} - yE_{Na} - (z/2)E_{O_2}$, where $E_{Ba_xNa_yO_z}$, E_{Ba}, E_{Na}, and E_{O_2} are the total energies for $Ba_xNa_yO_z$, *bcc*-Ba, *bcc*-Na, and α-O_2, respectively. The cyan circles indicate stable structures, while squares indicate metastable/unstable.

https://dx.doi.org/10.1021/jacs.9b13295
J. Am. Chem. Soc. 2020, 142, 5234−5240

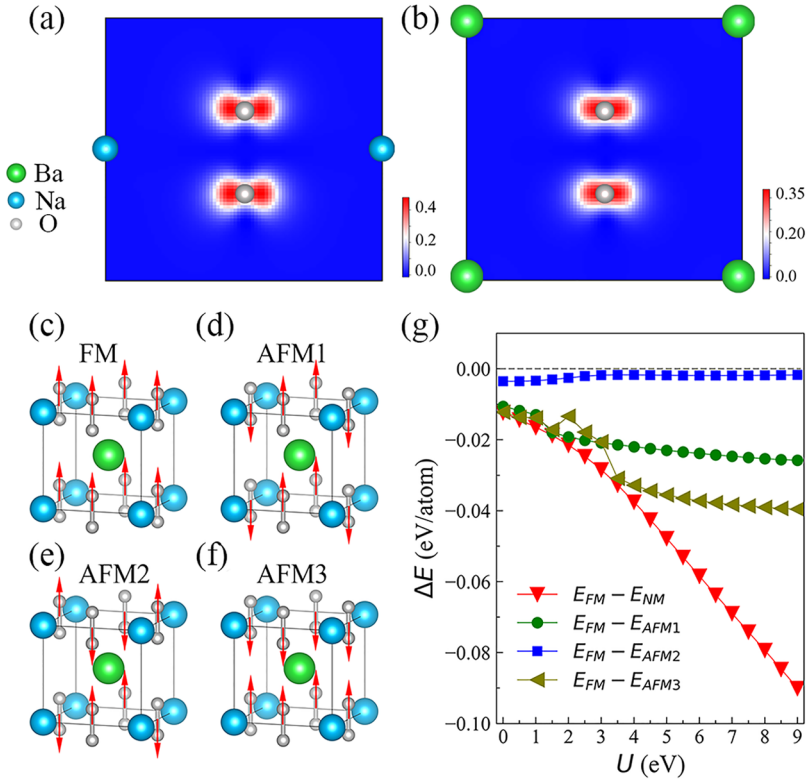

Figure 3. Magnetic density (electron/Å^3) of α-$BaNaO_4$ (a) (100) plane and (b) (200) plane. The magnetic density ρ_{mag} is defined as $\rho_{mag} = \rho_{up} - \rho_{down}$, where ρ_{up} is the charge density of spin-up electrons and ρ_{down} the charge density of spin-down electrons. (c−f) Four possible collinear magnetic configurations. (g) Energy differences between the FM and AFM1, AFM2, AFM3, and NM configurations as a function of U.

until all the forces on the ions were less than 10^{-4} eV/Å. The DFT+U method was used where mentioned. The Hubbard U is applied to the O-p orbitals. Phonon spectra were calculated using the finite displacement method implemented in the PHONOPY code[27] to determine the lattice dynamical stability of the structures. *Ab initio* molecular dynamics (AIMD) simulations were performed as implemented in VASP. The time step was chosen as 3 fs, and the duration was 9 ps. The hybrid functional HSE06 with a mixing parameter of 25% for the exact-exchange term was used to estimate the band gap in half-metals. We used the code from the Henkelman group[28] for Bader charge analysis. Structure searching and prediction were performed by using the particle swarm optimization (PSO) technique implemented in the CALYPSO code[29] in the Ba-Na-O system with molar ratio Ba:Na = 1:1.

■ RESULTS AND DISCUSSION

A structure search was performed on $BaNaO_x$ (x = 1−4). The corresponding structures with low energy and reasonable coordination geometry were singled out as candidates for further investigations. This yielded $P4/mmm$ α-$BaNaO_4$, $P4/mmm$ β-$BaNaO_4$, $P4/nmm$-BaNaO, $P\bar{1}$-$BaNaO_2$, $P4/mmm$-$BaNaO_2$, and $Pmmn$-$BaNaO_3$; see Figure 2a−f. We note that $P4/nmm$-BaNaO and $P4/mmm$-$BaNaO_2$ contain only O^{2-}, $P\bar{1}$-$BaNaO_2$ and $BaNaO_3$ have both O_2 dimers and O^{2-}, and α- and β-$BaNaO_4$ have only O_2 dimers. β-$BaNaO_4$ resembles BaO_2 in structure except for the Ba at the body center being substituted by Na, which is added for comparison. α-$BaNaO_4$ can be regarded as an O_2-dimer-deficient perovskite with a zero occupation of the dimer in the Ba layer. The O_2 dimers form a layer by bonding with Na^+ ions in the (001) plane, and the layers stack in a head-to-head way along the [001] direction, separated by Ba^{2+} ions. We notice that O-deficient perovskites are often seen in Cu-based superconductors.

Convex hull analyses of formation enthalpy were then performed to check the stability of these compounds by comparison with the known compounds in the Ba-Na-O ternary system. Figure 2g shows the calculated phase diagram. Only α-$BaNaO_4$ is stable in terms of formation energy. Others lie above the convex hull, suggesting they are unstable or metastable. We further explore the behavior of α-$BaNaO_4$ in terms of the lattice's dynamic, mechanical, and thermal stability. As there are no negative frequencies in the calculated phonon spectrum, its lattice is dynamically stable; see Figure S1 (Supporting Information, SI). For a stable compound, its elastic stiffness constants should satisfy the Born stability criteria.[30] The calculated stiffness values of α-$BaNaO_4$ are found to well guarantee the demand of mechanical stability (see details in the SI). Furthermore, the structural stability at 500 K was examined through AIMD. During the simulation process (0−9 ps), the structure is well preserved in the framework of the Nosé−Hoover thermostat ensemble; see Figure S2 (SI). Hence, the structure of α-$BaNaO_4$ is at least stable up to 500 K.

As is well known, prediction of the ground state of molecular magnetism in some compounds—in particular, in strongly electron correlated compounds—often fails if using local density approximation (LDA) and GGA as exchange correlation potentials. Using GGA+U, the magnetic ground state can be correctly reproduced if U is properly adopted;[10,17,18,21,31,32] here U is the electron correlation energy. RbO_2 is such a compound. Only when U is properly taken into account can its electronic and magnetic structures be calculated to be in good agreement with the experimental results. We follow this route and see whether this treatment can reproduce the right ground state. Our result shows that

https://dx.doi.org/10.1021/jacs.9b13295
J. Am. Chem. Soc. 2020, 142, 5234−5240

with $U < 4.5$ eV the ground state is FM half-metal, while with $U \geq 4.5$ eV we got the right AFM insulating state (Figure S3, SI) without setting any constraint on symmetry, as suggested in ref 17. Therefore, using GGA+U is an effective way to determine the magnetic ground state in O_2 dimer systems. Next, for α-$BaNaO_4$, we need to know: (1) whether a moment resides in each O_2 dimer, (2) how these moments order in the ground state, and (3) what is the ordering temperature?

To this end, we did spin polarization calculations for α-$BaNaO_4$ with a PBE functional and found that α-$BaNaO_4$ is a half-metal; see Figure S4a (SI). The magnetic density, i.e., the difference between spin-up and spin-down electrons, indicates that magnetic moments of α-$BaNaO_4$ originate from the O_2 dimers; see Figure 3a,b. The energies for non-magnetic (NM), FM, and three other possible AFM configurations (see Figure 3c−f) are then calculated against a series of U values. Figure 3g indicates that the FM configuration is the most favored state over all others, including the NM state from $U = 0$ to $U = 9$ eV. These results answer questions (1) and (2). Hence, α-$BaNaO_4$ is a ferromagnet in its ground state.

To answer question (3), we resort to Monte Carlo simulations based on the classical Heisenberg model. The Hamiltonian is written as $H = \sum_{ij} J_1 M_i M_j - \sum_{kl} J_2 M_k M_l - A\sum_i (s^z)^2$, where J_1 and J_2 are the first and second nearest-neighbor exchange coupling constants (see the inset of Figure 4), and A is the anisotropy energy parameter. J_1 and J_1 are

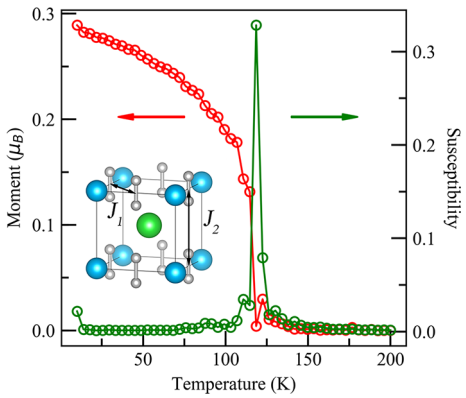

Figure 4. Temperature-dependent average magnetic moment and magnetic susceptibility based on Monte Carlo simulations. The inset shows an indication of exchange interaction for the nearest-neighbor J_1 and next-nearest-neighbor J_2.

extracted from Figure 3g by using different energies of magnetic ordering. A is extracted from the calculations on varying spin orientations (see details in the SI). The obtained J_1, J_2, and A are 36.9, 15.9, and 0.243 meV, respectively. Positive J_1 and J_2 indicate the coupling is FM. Figure 4 shows the variation of magnetic moment and magnetic susceptibility with respect to temperature. The magnetic moment decreases with increasing temperature and reaches zero at 120 K. A peak appearing at this temperature in the susceptibility indicates that T_c is about 120 K.

Like 3d and 4f metals, the local moment carried by an O_2 dimer is due to the unpaired electron in each π^* orbital. For α-$BaNaO_4$, 0.5 electron is expected to be absent in its two π^* orbitals for each O_2 dimer. In this case, the spins are very likely to polarize. Figure 5a,b shows the spin-resolved band structures calculated with an HSE06 hybrid functional. In the spin-up subband, a band gap of ∼4 eV separates the valence band, consisting of fully occupied π^* orbitals, and the fully empty conduction band of the σ^* orbital. In contrast, in the spin-down subband, the energy dispersions of unpaired electrons in the π^* orbitals cross the Fermi energy, resulting in a metallic feature. This is a typical half-metal. The partial density of states (Figure 5c) confirms that the states near the Fermi level predominantly come from the O-2p orbitals. The states from the Na and Ba lie far away from the Fermi level, indicating there is nearly no orbital hybridization between O and Na/Ba. α-$BaNaO_4$ is essentially an ionic compound.

More specifically, the Bader charge analysis indicates that Ba loses 1.58 e^-, Na loses 0.87 e^-, and the O_2 dimer gains 1.23 e^- on average. Hence, the average valence state of O_2 should be written as $O_2^{1.5-}$, considering the charge neutrality requirement. Figure 5d−g shows the charge density for the bands labeled in Figure 5a. Obviously, the p_z−p_z orbitals of the O_2 dimer form the σ and σ^* bonds, and side-to-side overlap of the p_x−p_x and p_y−p_y orbitals forms the π and π^* bonds. The molecular O_2 feature is still preserved. Figure 5h depicts schematically the hybridization of the O_2 dimer. In the spin-up subband, π^* bands are fully occupied by two electrons. It should be noted that, in the spin-down subband, π^* bands are only occupied by an average of 1.5 e^-/dimer. In this way, the magnetic moment per O_2 dimer should be 0.5 μ_B, consistent with the calculated magnetic moment of 1 μ_B/cell (two dimers per cell). Such an integer moment is another character of half-metals.

Kim et al. argued that spin−orbit coupling (SOC) along with Coulomb correlation will open a gap in the metallic channel of the FM configuration KO_2.[21] We examine this effect on the band structure of α-$BaNaO_4$ by using GGA, GGA+U, GGA+SOC, and GGA+U+SOC as the exchange corrections. Our results found that small shifts or disappearances of degeneracy in dispersions are observed for some K points; see Figure S4. Therefore, the half-metallicity of α-$BaNaO_4$ originates from partially filled π^* bonds, and SOC is not indispensable here.

We examine the robustness of the FM ordering under certain strains. The strain was mimicked by changing the lattice parameters, a and c, with a ratio χ, where a negative χ indicates compressive strain, and a positive χ indicates tensile strain. The atomic positions are then optimized against the new parameters. As depicted in Figure 6, when compressive strain is applied, the magnetic moment remains almost unchanged within 6% strain and then rapidly decreases. The half-metallicity will disappear because the moments are less than 1 μ_B, violating the requirement of integer moment. Meanwhile, the bond length of O−O varies from 1.427 to 1.393 Å. Moreover, at a compressive strain up to 20%, the O_2 dimers become much shorter, ∼1.340 Å, and non-magnetic. Similar cases are observed for SrN and SrN_2, where SrN owns magnetic moments with a proper bond length for the N_2 dimer, while SrN_2 is non-spin-polarized with a shorter bond length.[33] So, the bond length of the O_2 dimer is highly relevant to the appearance of polarized spins. After applying tensile strains within 10%, the FM holds against three AFM and NM configurations, and the half-metallic feature remains. This means that the half-metallicity is more sensitive to compressive than to tensile strains for α-$BaNaO_4$.

The ferromagnetic ordering of α-$BaNaO_4$ could be explained by the coexistence of double exchange and direct exchange interactions. Its chemical formula can be written as $Ba^{2+}Na^{+}O_2^{2-}O_2^{-}$, i.e., mixed-valent O_2^{2-} and O_2^{-} anions

https://dx.doi.org/10.1021/jacs.9b13295
J. Am. Chem. Soc. 2020, 142, 5234−5240

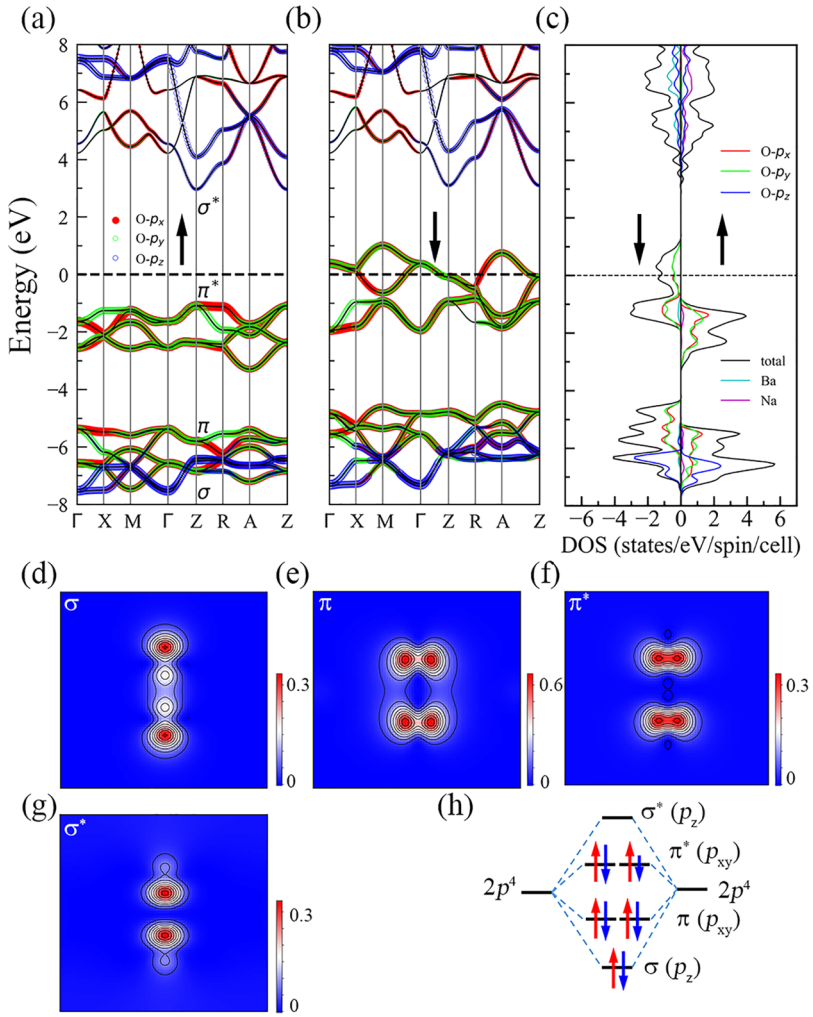

Figure 5. Spin and orbital resolved band structures of α-$BaNaO_4$ for (a) spin-up subband and (b) spin-down subband with an HSE06 hybrid functional, where the Fermi level was set to be zero. Red circles indicate O-p_x orbitals, green O-p_y orbitals, and blue O-p_z orbitals. The contributions of the orbitals are proportional to the size of the circle. (c) Orbital-resolved density of states contributions from Ba, Na, and O atoms in α-$BaNaO_4$. (d−g) Charge density of the (100) plane for the bands labeled in (a). (h) Schematic representation of hybridization of the O_2 dimer. Note here that the extra 1.5 electrons are donated from the Ba and Na atoms.

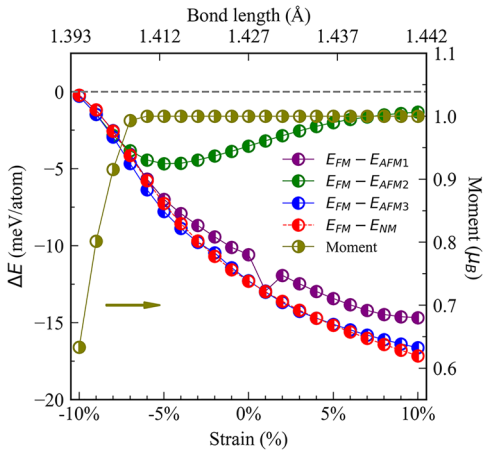

Figure 6. Magnetic moment of FM configuration and energy difference between AFM1, AFM2, AFM3, NM, and FM vary with strain. The upper axis shows the corresponding bond length of the O_2 dimer at different strains.

coexist. Similar to $La_{1-x}A_xMnO_3$ (A = Ca, Sr, Ba), where the electron hops from Mn^{3+} to Mn^{4+} through double exchange,[34] the itinerant electrons in the π^* orbitals could hop from O_2^{2-} to O_2^- in the (001) plane mediated by Na^+ ions, guaranteeing the spins are parallel.[20] Along the [001] direction, a positive J_2 could be explained as FM interaction through direct exchange interactions among the head-to-head O_2 dimers. All neighboring O_2-dimer layers are coupled ferromagnetically as expected.

α-$BaNaO_4$ is different from the known O_2-dimer-containing compounds in both structure and magnetic properties. First, the orientation of O_2 dimers is a key factor. If they do not align in one direction, it is hard to form long-range magnetic ordering. That is the cases for Rb_4O_6 and Cs_4O_6, where the O_2 dimers do not align in an identical orientation, leading to frustrated magnetism.[10,11] Second, the coupling type between O_2 dimers is important. Although the dimers align along one direction in AO_2 (A = K, Rb, Cs), they show AFM orderings because of inter-AFM coupling between adjacent planes.[21] In α-$BaNaO_4$, the adjacent planes couple ferromagnetically through direct interactions. The coupling switch is attributed to the difference ways O_2 dimer layers stack: a shift (0.5a, 0.5a, 0) between adjacent planes for the former compounds and

https://dx.doi.org/10.1021/jacs.9b13295
J. Am. Chem. Soc. 2020, 142, 5234−5240

head-to-head along the c direction for the latter. So, the direct-exchange interaction between adjacent O_2 dimers along the c-axis plays a vital role in the formation of ferromagnetic ordering. To check this, we shift the middle layer in AFM RbO_2 with a vector (0.5a, 0.5a, 0) within the unit cell, and the resultant arrangement of O_2 dimers between the adjacent layers is head-to-head; see Figure S5 (SI). In this geometry, the calculated ground state changes into FM when U = 6.5 eV. It should be noted that, in a tetragonal structure, the O_2 dimer layers are allowed to have only these two configurations.

At low temperatures, AO_2 (A = K, Rb, Cs) usually undergo several structural transitions, where the O_2 dimers would slightly incline with a small angle to lift the degeneracy of π^* orbitals.[4,5] To clarify the influence of tilted O_2 dimers on the magnetic property, O_2 dimers in α-$BaNaO_4$ were rotated by 30°. As suggested in ref 21, two kinds of tilted structures were considered: type [R1], in which the O_2 dimers are 30° off the z axis in the xz plane, see Figure S6a,b; and type [R2], in which the O_2 dimers are 30° off the z axis in the (110) plane, see Figure S6c,d. We compared the total energies of different magnetic states. It shows the inclination of O_2 dimers do not influence the ground state of α-$BaNaO_4$ with U = 6.5 eV or without U, see Table S2 in the SI. The FM ordering still survives.

Although other predicted structures are not energy favorable, but $P4/nmm$-BaNaO and $P\bar{1}$-$BaNaO_2$ are stable in terms of lattice dynamics and mechanical dynamics, see details in the SI. We also examine their properties. They do not show spin-polarized behavior. $P4/nmm$-BaNaO is a non-magnetic metal, and $P\bar{1}$-$BaNaO_2$ is a semiconductor; see Figures S7(a) and S8. It should be noted that $P4/nmm$-BaNaO, whose chemical formula could be written as Ba^{2+} Na^+ $O^{2-}\cdot e^-$. The electrons were confined between the empty space formed by Na^+ ions; see Figure S7b. It may be a potential electride material,[35] which deserves further investigation.

We note that N_2 dimers can also induce magnetism in some nitrides if there exist unpaired electrons in its π^*orbitals, such as SrN.[33] Besides, N_2 dimers were predicted to form other nitrides with main group element and 3d metals, which can be a metal with excellent thermal and electrical conductivity for SiN_4[36] and a half-metal for FeN_4.[37] More novel magnetic and other emergent properties are expected in these compounds containing O_2 and N_2 dimers.[38] Hayyan and co-workers recently gave a very comprehensive review on the generation and implications of O_2^-.[39] This will be helpful in synthesizing the molecule oxygen containing compounds, including these ternary ones.

CONCLUSION

In summary, by first-principles calculations, we show that α-$BaNaO_4$ is a half-metal. It is energetically favorable, and its lattice is dynamically, mechanically, and thermally stable. It possesses robust FM ordering with a T_c of 120 K. The partially occupied π^* orbitals in the metallic channel and fully occupied π^* orbitals in the semiconducting channel is the origin of half-metallicity. Unlike previously reported AO_2 (A = K, Rb, Cs) with AFM orderings between (001) layers through indirect exchange interactions, the O_2 dimer layers in α-$BaNaO_4$ coupled ferromagnetically to each other through direct interactions, with head-to-head alignment along the [001] direction. Our work provides new insights in exploring the FM and half-metallicity in O_2-dimer-containing compounds.

ASSOCIATED CONTENT

Supporting Information

The Supporting Information is available free of charge at https://pubs.acs.org/doi/10.1021/jacs.9b13295.

Lattice parameters; elastic constants; details of estimation coupling constant; phonon spectra and band structures of $BaNaO_x$; molecular dynamics simulations of $BaNaO_4$; more band structure results of $BaNaO_4$; shifted configuration of RbO_2; structures and formation enthalpies of related compounds (PDF)

AUTHOR INFORMATION

Corresponding Authors

Jiangang Guo − *Beijing National Laboratory for Condensed Matter Physics, Institute of Physics, Chinese Academy of Sciences, Beijing 100190, China; Songshan Lake Materials Laboratory, Dongguan, Guangdong 523808, China;* orcid.org/0000-0003-3880-3012; Email: jgguo@iphy.ac.cn

Xiaolong Chen − *Beijing National Laboratory for Condensed Matter Physics, Institute of Physics, Chinese Academy of Sciences, Beijing 100190, China; School of Physical Sciences, University of Chinese Academy of Sciences, Beijing 101408, China; Songshan Lake Materials Laboratory, Dongguan, Guangdong 523808, China;* orcid.org/0000-0001-8455-2117; Email: chenx29@iphy.ac.cn

Author

Jun Deng − *Beijing National Laboratory for Condensed Matter Physics, Institute of Physics, Chinese Academy of Sciences, Beijing 100190, China; School of Physical Sciences, University of Chinese Academy of Sciences, Beijing 101408, China*

Complete contact information is available at: https://pubs.acs.org/10.1021/jacs.9b13295

Notes

The authors declare no competing financial interest.

ACKNOWLEDGMENTS

This work is financially supported by the MoST-Strategic International Cooperation in Science, Technology and Innovation Key Program (2018YFE0202601); National Natural Science Foundation of China under Grants No. 51922105, 51532010, and 51772322; the National Key Research and Development Program of China (2016YFA0300600, 2017YFA0304700); and the Key Research Program of Frontier Sciences, CAS, Grant No. QYZDJ-SSW-SLH013.

REFERENCES

(1) Kanda, E.; Haseda, T.; Ötsubo, A. Paramagnetic susceptibility of solid oxygen. *Physica* **1954**, *20* (1), 131−132.

(2) Meier, R. J.; Helmholdt, R. B. Neutron-diffraction study of α- and β-oxygen. *Phys. Rev. B: Condens. Matter Mater. Phys.* **1984**, *29* (3), 1387−1393.

(3) Morris, G. D.; Brewer, J. H.; Dunsiger, S. R.; Montour, M. Antiferromagnetism in solid oxygen. *Hyperfine Interact.* **1997**, *104* (1−4), 381−385.

(4) Labhart, M.; Raoux, D.; Känzig, W.; Bösch, M. A. Magnetic order in 2p-electron systems: Electron paramagnetic resonance and antiferromagnetic resonance in the alkali hyperoxides KO_2, RbO_2, and CsO_2. *Phys. Rev. B: Condens. Matter Mater. Phys.* **1979**, *20* (1), 53−70.

(5) Astuti, F.; Miyajima, M.; Fukuda, T.; Kodani, M.; Nakano, T.; Kambe, T.; Watanabe, I. Anionogenic Magnetism Combined with Lattice Symmetry in Alkali-metal Superoxide RbO_2. *J. Phys. Soc. Jpn.* **2019**, *88* (4), 043701.
(6) Smith, H. G.; Nicklow, R. M.; Raubenheimer, L. J.; Wilkinson, M. K. Antiferromagnetism in potassium superoxide KO_2. *J. Appl. Phys.* **1966**, *37* (3), 1047−1049.
(7) Hesse, W.; Jansen, M.; Schnick, W. Recent results in solid state chemistry of ionic ozonides, hyperoxides, and peroxides. *Prog. Solid State Chem.* **1989**, *19* (1), 47−110.
(8) Ylvisaker, E. R.; Singh, R. R. P.; Pickett, W. E. Orbital order, stacking defects, and spin fluctuations in the *p*-electron molecular solid RbO_2. *Phys. Rev. B: Condens. Matter Mater. Phys.* **2010**, *81* (18), 180405.
(9) Sparks, J. T.; Komoto, T. Magnetic properties of NaO_2 and KO_2. *J. Appl. Phys.* **1966**, *37* (3), 1040−1041.
(10) Winterlik, J.; Fecher, G. H.; Felser, C.; Mühle, C.; Jansen, M. Challenging the prediction of anionogenic ferromagnetism for Rb_4O_6. *J. Am. Chem. Soc.* **2007**, *129* (22), 6990−6991.
(11) Winterlik, J.; Fecher, G. H.; Jenkins, C. A.; Medvedev, S.; Felser, C.; Kübler, J.; Mühle, C.; Doll, K.; Jansen, M.; Palasyuk, T.; Trojan, I.; Eremets, M. I.; Emmerling, F. Exotic magnetism in the alkali sesquioxides Rb_4O_6 and Cs_4O_6. *Phys. Rev. B: Condens. Matter Mater. Phys.* **2009**, *79* (21), 214410.
(12) Kim, M.; Min, B. I. Mott physics in the 2*p* electron dioxygenyl magnet O_2MF_6 (*M* = Sb, Pt). *Phys. Rev. B: Condens. Matter Mater. Phys.* **2011**, *84* (7), 073106.
(13) DiSalvo, F. J.; Falconer, W. E.; Hutton, R. S.; Rodriguez, A.; Waszczak, J. V. A study of magnetic state of O_2^+ in fluoride salts. *J. Chem. Phys.* **1975**, *62* (7), 2575−2580.
(14) Giriyapura, S.; Zhang, B.; de Groot, R. A.; de Wijs, G. A.; Caretta, A.; van Loosdrecht, P. H. M.; Kockelmann, W.; Palstra, T. T. M.; Blake, G. R. Anionogenic Mixed Valency in $K_xBa_{1-x}O_{2-\delta}$. *Inorg. Chem.* **2014**, *53* (1), 496−502.
(15) Giriyapura, S. Mixed valency and anionogenic magnetism in alkali metal oxides. Ph.D. Thesis, University of Groningen, Groningen, The Netherlands, November 2012; http://irs.ub.rug.nl/ppn/35216378X.
(16) Riyadi, S.; Giriyapura, S.; de Groot, R. A.; Caretta, A.; van Loosdrecht, P. H. M.; Palstra, T. T. M.; Blake, G. R. Ferromagnetic Order from *p*-Electrons in Rubidium Oxide. *Chem. Mater.* **2011**, *23* (6), 1578−1586.
(17) Kováčik, R.; Ederer, C. Correlation effects in *p*-electron magnets: Electronic structure of RbO_2 from first principles. *Phys. Rev. B: Condens. Matter Mater. Phys.* **2009**, *80* (14), 140411.
(18) Kim, M.; Min, B. I. Temperature-dependent orbital physics in a spin-orbital-lattice-coupled 2*p* electron Mott system: The case of KO_2. *Phys. Rev. B: Condens. Matter Mater. Phys.* **2014**, *89* (12), 121106.
(19) Naghavi, S.; Chadov, S.; Felser, C.; Fecher, G. H.; Kübler, J.; Doll, K.; Jansen, M. Pressure induced insulator/half-metal/metal transition in a strongly correlated *p*-electron system. *Phys. Rev. B: Condens. Matter Mater. Phys.* **2012**, *85* (20), 205125.
(20) Zhang, B.; Cao, C.; Li, G.; Li, F.; Ji, W.; Zhang, S.; Ren, M.; Zhang, H.; Zhang, R.-Q.; Zhong, Z.; Yuan, Z.; Yuan, S.; Blake, G. R. 2*p*-insulator heterointerfaces: Creation of half-metallicity and anionogenic ferromagnetism via double exchange. *Phys. Rev. B: Condens. Matter Mater. Phys.* **2018**, *97* (16), 165109.
(21) Kim, M.; Kim, B. H.; Choi, H. C.; Min, B. I. Antiferromagnetic and structural transitions in the superoxide KO_2 from first principles: A 2*p*-electron system with spin-orbital-lattice coupling. *Phys. Rev. B: Condens. Matter Mater. Phys.* **2010**, *81* (10), 100409.
(22) Cao, Y.; Fatemi, V.; Fang, S.; Watanabe, K.; Taniguchi, T.; Kaxiras, E.; Jarillo-Herrero, P. Unconventional superconductivity in magic-angle graphene superlattices. *Nature* **2018**, *556* (7699), 43−50.
(23) Kresse, G.; Furthmüller, J. Efficiency of ab-initio total energy calculations for metals and semiconductors using a plane-wave basis set. *Comput. Mater. Sci.* **1996**, *6* (1), 15−50.
(24) Perdew, J. P.; Burke, K.; Ernzerhof, M. Generalized gradient approximation made simple. *Phys. Rev. Lett.* **1996**, *77* (18), 3865−3868.
(25) Kresse, G.; Joubert, D. From ultrasoft pseudopotentials to the projector augmented-wave method. *Phys. Rev. B: Condens. Matter Mater. Phys.* **1999**, *59* (3), 1758.
(26) Monkhorst, H. J.; Pack, J. D. Special points for Brillouin-zone integrations. *Phys. Rev. B: Condens. Matter Mater. Phys.* **1976**, *13* (12), 5188−5192.
(27) Togo, A.; Tanaka, I. First principles phonon calculations in materials science. *Scr. Mater.* **2015**, *108*, 1−5.
(28) Tang, W.; Sanville, E.; Henkelman, G. A grid-based Bader analysis algorithm without lattice bias. *J. Phys.: Condens. Matter* **2009**, *21* (8), 084204.
(29) Wang, Y.; Lv, J.; Zhu, L.; Ma, Y. Crystal structure prediction via particle-swarm optimization. *Phys. Rev. B: Condens. Matter Mater. Phys.* **2010**, *82* (9), 094116.
(30) Wu, Z.-j.; Zhao, E.-j.; Xiang, H.-p.; Hao, X.-f.; Liu, X.-j.; Meng, J. Crystal structures and elastic properties of superhard IrN_2 and IrN_3 from first principles. *Phys. Rev. B: Condens. Matter Mater. Phys.* **2007**, *76* (5), 054115.
(31) Attema, J. J.; de Wijs, G. A.; Blake, G. R.; de Groot, R. A. Anionogenic ferromagnets. *J. Am. Chem. Soc.* **2005**, *127* (46), 16325−16328.
(32) Winterlik, J.; Fecher, G. H.; Jenkins, C. A.; Felser, C.; Mühle, C.; Doll, K.; Jansen, M.; Sandratskii, L. M.; Kübler, J. Challenge of Magnetism in Strongly Correlated Open-Shell 2*p* Systems. *Phys. Rev. Lett.* **2009**, *102* (1), 016401.
(33) Volnianska, O.; Boguslawski, P. Molecular magnetism of monoclinic SrN: A first-principles study. *Phys. Rev. B: Condens. Matter Mater. Phys.* **2008**, *77* (22), 220403.
(34) Goodenough, J. B. Theory of the role of covalence in the perovskite-type manganites [La, *M*(II)]MnO_3. *Phys. Rev.* **1955**, *100* (2), 564−573.
(35) Tada, T.; Takemoto, S.; Matsuishi, S.; Hosono, H. High-Throughput ab Initio Screening for Two-Dimensional Electride Materials. *Inorg. Chem.* **2014**, *53* (19), 10347−10358.
(36) Liu, N.; Chen, X.; Guo, J.; Deng, J.; Guo, L. New Type of Nitrides with High Electrical and Thermal Conductivities. *Chin. Phys. Lett.* **2018**, *35* (8), 087102.
(37) Deng, J.; Liu, N.; Guo, J.; Chen, X. Large spin gaps in the half-metals MN_4 (*M*=Mn, Fe, Co) with N_2 dimers. *Phys. Rev. B: Condens. Matter Mater. Phys.* **2019**, *99* (18), 184409.
(38) Volnianska, O.; Boguslawski, P. Magnetism of solids resulting from spin polarization of *p* orbitals. *J. Phys.: Condens. Matter* **2010**, *22* (7), 073202.
(39) Hayyan, M.; Hashim, M. A.; AlNashef, I. M. Superoxide Ion: Generation and Chemical Implications. *Chem. Rev.* **2016**, *116* (5), 3029−3085.

https://dx.doi.org/10.1021/jacs.9b13295
J. Am. Chem. Soc. 2020, 142, 5234−5240